Synthesis and characterization of two new classes of ruthenium(III)–sulfoxide complexes with nitrogen donor ligands (L): Na[*trans*-$RuCl_4(R_2SO)(L)$] and *mer,cis*-$RuCl_3(R_2SO)(R_2SO)(L)$. The crystal structure of Na[*trans*-$RuCl_4(DMSO)(NH_3)]\cdot 2DMSO$, Na[*trans*-$RuCl_4(DMSO)(Im)]\cdot H_2O,Me_2CO$ (Im = imidazole) and *mer,cis*-$RuCl_3(DMSO)(DMSO)(NH_3)$

E. Alessio*, G. Balducci, A. Lutman, G. Mestroni, M. Calligaris and W. M. Attia**
Dipartimento di Scienze Chimiche, Università di Trieste, 34127 Trieste (Italy)

(Received June 16, 1992; revised August 21, 1992)

Abstract

In this paper we report the synthesis of two new classes of chloride–sulfoxide–Ru(III) derivatives containing a nitrogen ligand (L) of general formula: Na[*trans*-$RuCl_4(R_2SO)(L)$] and *mer,cis*-$RuCl_3(R_2SO)(R_2SO)(L)$. Their spectroscopic characterization in the solid state (IR) and in solution (NMR, UV–Vis) is also described. The cyclic voltammetry of the complexes performed in aqueous solution shows in every case a monoelectronic and rather rapid Ru(III)/Ru(II) electron transfer. The observed formal potentials are much more positive than those reported for other Ru(III) complexes. The net charge, together with the π acidic ability of DMSO, are the factors responsible for this behaviour. The crystal structures of Na[*trans*-$RuCl_4(DMSO)(NH_3)]\cdot 2DMSO$ (**5a**), Na[*trans*-$RuCl_4(DMSO)(Im)]\cdot H_2O,Me_2CO$ (**5b**) and *mer,cis*-$RuCl_3(DMSO)(DMSO)(NH_3)$ (**6a**) have been determined by three dimensional X-ray analyses. Crystal data are: $a = 9.578(2)$, $b = 12.480(2)$, $c = 9.594(6)$ Å, $\alpha = 104.33(3)$, $\beta = 119.04(2)$, $\gamma = 80.71(3)°$, triclinic, space group $P\bar{1}$, $Z = 2$ for **5a**; $a = 10.790(4)$, $b = 11.411(4)$, $c = 7.658(4)$ Å, $\alpha = 105.92(3)$, $\beta = 93.61(1)$, $\gamma = 83.50(3)°$, triclinic, space group $P\bar{1}$, $Z = 2$ for **5b**; $a = 10.110(3)$, $b = 9.718(3)$, $c = 14.101(3)$ Å, $\beta = 108.89(3)°$, monoclinic, space group $P2_1/n$, $Z = 4$ for **6a**. Least-squares refinement based on 4897 (**5a**), 4932 (**5b**) and 3152 (**6a**) independent reflections converged to $R = 0.039$, 0.031 and 0.022, respectively. In **5a** and **5b**, the DMSO ligand is S-bonded to Ru, with Ru–S bond distances (*trans* to N) of 2.2797(7) and 2.2956(6) Å, respectively, while in **6a**, one DMSO, *trans* to N, is S-bonded (Ru–S, 2.2714(6) Å), and the other, *trans* to Cl, is O-bonded (Ru–O, 2.070(2) Å). The Ru–Cl bond distance, *trans* to O, is 2.3207(7) Å. The Ru–Cl bond distances, *trans* to Cl, are similar in all three compounds averaging 2.343(6) Å. Relevance in the synthesis of the new derivatives comes from the known antitumor properties of isostructural Ru(III) complexes with heterocyclic nitrogen ligands. The antitumor activity of some of the new compounds are currently under investigation. Their redox potentials suggest the possibility that they might undergo an easy biological reduction *in vivo*.

Introduction

Several reports concerning halogen–dimethyl sulfoxide–ruthenium(III) complexes have been published since the pioneering work of Wilkinson's group describing a complex of formula $RuCl_3(DMSO)_3$ [1]. However, none of the proposed compounds had been unambiguously characterized [1–4]. To our knowledge and personal experience, most of the syntheses reported either could not be reproduced [5] or gave compounds that, when correctly characterized, resulted different from those expected [6, 7].

Only very recently two independent publications [6, 8] reported the synthesis and crystal structure of a chloride–dimethyl sulfoxide–ruthenium(III) compound, namely $[(DMSO)_2H][trans\text{-}RuCl_4(DMSO)_2]$ (**1**)†. We also described the synthesis and structural characterization of complexes such as [(Acr)H][*trans*-$RuCl_4(DMSO)_2$] (Acr = acridine) [9] and *mer*-$RuCl_3(DMSO)_2(DMSO)$ (**2**) [8] and of similar anionic and neutral compounds with tetramethylene sulfoxide

*Author to whom correspondence should be addressed.
**On leave from the Physics Department, Suez Canal University, Ismailia, Egypt.

†DMSO = S-bonded dimethyl sulfoxide; DMSO = O-bonded dimethyl sulfoxide.

0020-1693/93/$6.00

(TMSO): [(TMSO)H][*trans*-$RuCl_4(TMSO)_2$] (**3**) and *mer*-$RuCl_3(TMSO)_2(TMSO)$ (**4**) [10]. In the anionic derivatives, the protonated sulfoxide can be easily replaced by Na^+ to give the corresponding sodium salts **1Na** [8] and **3Na**.

Our interest in ruthenium–sulfoxide compounds derives mainly from their potentialities in the field of non-platinum inorganic antitumor drugs [11] and we have been investigating both the 2+ [10, 12–14] and 3+ [8, 10, 15] ruthenium oxidation states. In this perspective, the ruthenium(III)–sulfoxide complexes **1–4** appeared particularly attractive, being structurally very similar to the Ru(III) compounds with heterocyclic nitrogen donor ligands, such as [(Im)H][*trans*-$RuCl_4(Im)_2$] (Im = imidazole) (**ICR**) reported by Keppler's group as being quite active against platinum resistant colorectal tumor models [16]. In fact, the anionic compounds are isostructural and isoelectronic to **ICR**, with S-bonded sulfoxides sitting in the place of the nitrogen ligands.

The ruthenium–sulfoxide complexes proved, however, to be rather labile in aqueous solution [8, 10, 15], in particular at physiological pH where they are readily hydrolyzed. With the aim of tailoring new ruthenium(III)–sulfoxide complexes with improved inertness in aqueous solution, we synthesized from the precursors **1–4** two new classes of ruthenium(III) compounds of general formula Na[*trans*-$RuCl_4(R_2SO)(L)$] (**5**, R_2SO = DMSO; **7**, R_2SO = TMSO) and *mer,cis*-$RuCl_3(R_2SO)(R_2SO)(L)$ (**6**, R_2SO = DMSO; **8**, R_2SO = TMSO), with L = nitrogen donor ligand. In this paper we describe their synthesis and structural characterization, based on spectroscopic results and supported by the crystal structures of the two anionic derivatives, Na[*trans*-$RuCl_4(DMSO)(NH_3)]\cdot 2DMSO$ (**5a**) and Na[*trans*-$RuCl_4(DMSO)(Im)]\cdot H_2O,Me_2CO$ (**5b**) and of the neutral compound *mer,cis*-$RuCl_3(DMSO)(DMSO)(NH_3)]$ (**6a**).

In order to explain the antitumor activity of inert Ru(III) complexes, an 'activation by reduction' mechanism has been proposed [17]. According to this hypothesis, an *in situ* Ru(III)/Ru(II) reduction would produce more labile species, which should be able to interact with biological targets after dissociation of some ligands. A biologically accessible redox potential is obviously required for a complex in order to fit in such mechanism. In this perspective, we determined the redox potentials of the complexes in order to ascertain the feasibility of their biological reduction.

Finally, as reported by the group of James [18] ruthenium–sulfoxide complexes might also find applications in the field of medicinal chemistry as radiosensitizers, when properly substituted with nitroimidazole ligands. The new classes of compounds here described might therefore open interesting perspectives also in this field.

Experimental

Materials

Analytical grade dimethyl sulfoxide (C. Erba), solvents (Baker) and ligands (Aldrich) were used without further purification for synthetic purposes. Commercial $RuCl_3\cdot 3H_2O$ was purchased from Johnson Matthey. DMSO-d_6 and D_2O were purchased from Cambridge Isotope Laboratories. Doubly distilled water and analytical grade $NaClO_4\cdot 2H_2O$ were employed for the electrochemical experiments in aqueous solution.

Physical measurements

Electronic absorption spectra were recorded in stoppered quartz cells with a Perkin-Elmer Lambda 5 UV–Vis spectrophotometer equipped with a Haake F3 thermo-cryostat. Solid state IR spectra were recorded in KBr pellets on in nujol mull between CsI windows on a Perkin-Elmer 983G spectrometer.

^1H NMR spectra were obtained on a Nicolet 360 MHz spectrometer using a 12 μs 90° pulse over a 30 KHz bandwidth with 16K data points. All spectra were recorded in D_2O at room temperature with 3-(trimethylsilyl)tetradeutero sodium propionate (TSP) as internal standard.

Cyclic voltammetric measurements were performed under inert atmosphere (Ar) in a three electrode cell at 25.0 °C. The working electrode was a Pt bead obtained by melting the end of a Pt wire. The wire was sealed in a pipette in such a way that only the bead protruded out of the pipette tip. The counter electrode was a Pt wire coiled on the working electrode holder in order to improve the geometry of the cell arrangement. The reference electrode was a conventional NaCl saturated calomel electrode (SSCE) and all the potentials are referred to it, unless explicitly stated; it was fitted in a Luggin probe filled with the same solution used for the measurements. The working electrode was cleaned immediately prior to use by heating it to whiteness on an oxy-gas micro flame.

The electrochemical instrumentation included a home built potentiostat equipped with 'damped' positive feedback for *iR* compensation [19], an Amel 568 function generator and a Nicolet 2090IIIa digital oscilloscope. The digitized cyclic voltammetric traces were transferred to an IBM PS/2 personal computer and numerically processed.

Synthesis of the complexes

[$(DMSO)_2H$][*trans*-$RuCl_4(DMSO)_2$] (**1**), Na[*trans*-$RuCl_4(DMSO)_2$] (**1Na**) and *mer*-$RuCl_3(DMSO)_2$-

(DMSO) (**2**), and the corresponding hexadeuterated derivatives were synthesized according to the procedures reported in ref. 8. The tetramethylene sulfoxide complexes [(TMSO)H][*trans*-$RuCl_4(TMSO)_2$] (**3**), Na[*trans*-$RuCl_4(TMSO)_2$] (**3Na**), and *mer*-$RuCl_3(TMSO)_2$-(TMSO) (**4**) were synthesized according to the procedures reported in ref. 10.

We describe here the synthesis of the anionic and neutral DMSO derivatives with ammonia (**5a** and **6a**, respectively) and imidazole (**5b** and **6b**, respectively). All the other compounds with different nitrogen donor ligands were synthesized with procedures very similar to those reported for the imidazole derivatives, adopting the same ligand to ruthenium ratio and solvent mixture. In the case of indazole and isoquinoline, also the anionic compounds are very soluble in cold acetone and therefore the precipitates were washed with diethyl ether only. The corresponding TMSO derivatives were synthesized according to very similar procedures, which are not reported here for the sake of brevity.

*Sodium trans-(dimethyl sulfoxide)(ammonia)tetrachloro ruthenate(III) (Na[trans-$RuCl_4$(DMSO)(NH_3)]) (**5a**)*

A 0.5 g amount of **1Na** (1.2 mmol) was partially dissolved in a mixture of 10 ml of acetone and 2 ml of DMSO in a flask closed with a stopcock. The flask was first connected to a vacuum line and then to a reservoir of gaseous ammonia. Within 1 min at r.t., under magnetic stirring, the reactant dissolved completely and the initially orange solution turned brown–yellow. The product rapidly precipitated from the solution as light orange microcrystals which, after 15 min, were filtered off, washed with cold acetone and diethyl ether, and vacuum dried at r.t. (yield 85%).

The complex contains two DMSO molecules of crystallization and can be better formulated as Na[*trans*-$RuCl_4$(DMSO)(NH_3)]·2DMSO, *Anal.* Calc. for Na[*trans*-$RuCl_4$(DMSO)(NH_3)]·2DMSO (M_r = 517.28): C, 13.9; H, 4.09; N, 2.70. Found: C, 14.5; H, 3.96; N, 2.66%.

Acetone and, sometimes, water molecules can partially replace the DMSO molecules of crystallization, thereby affecting the goodness and reproducibility of elemental analysis. The above reported analysis was probably affected by the presence of acetone as an impurity.

*Sodium trans-(dimethyl sulfoxide)(imidazole)tetrachlororuthenate(III) (Na[trans-$RuCl_4$(DMSO)(Im)]) (**5b**)*

A 0.6 g amount of **1Na** (1.4 mmol) was partially dissolved in a mixture of 10 ml of acetone and 2 ml of DMSO. 0.48 g of imidazole (7 mmol) dissolved in 4 ml of acetone was added to the mixture under magnetic stirring. After 15 min at r.t. the reactant dissolved almost completely and the solution was filtered over a fine paper filter. Orange–yellow crystals of the product formed from the clear solution after some hours at room temperature and were filtered off, washed with cold acetone and diethyl ether, and vacuum dried at r.t.. Crystal formation could be hastened and increased by addition of small amounts of diethyl ether (yield 80%).

As in the case of the ammonia derivative **5a**, the complex contains two DMSO molecules of crystallization and can be better formulated as Na[*trans*-$RuCl_4$(DMSO)(Im)]·2DMSO. *Anal.* Calc. for Na[*trans*-$RuCl_4$(DMSO)(Im)]·2DMSO (M_r = 568.32): C, 19.02; H, 3.90; N, 4.92. Found: C, 19.5; H, 3.87; N, 4.75%.

Also in this case, acetone and, sometimes, water molecules can partially replace the DMSO molecules of crystallization, thereby affecting the goodness and reproducibility of elemental analysis.

*mer-Trichlorobis(dimethyl sulfoxide)(ammonia)-ruthenium(III) (mer-$RuCl_3(DMSO)_2(NH_3)$) (**6a**)*

A 0.5 g amount of **2** (1.1 mmol) was dissolved in a mixture of CH_2Cl_2 (7 ml) and DMSO (0.5 ml) in a flask closed with a stopcock. The flask was first connected to a vacuum line and then to a reservoir of gaseous ammonia. In a few minutes at r.t. the solution turned from red to brown–yellow and microcrystals of the same color began to form. After 30 min they were filtered off, washed with cold CH_2Cl_2 and diethyl ether, and vacuum dried at r.t. (yield 85%). *Anal.* Calc. for $RuCl_3(DMSO)_2(NH)_3$ (M_r = 380.75): C, 12.62; H, 3.97; N, 3.67. Found: C, 12.7; H, 3.95; N, 3.47%.

*mer-Trichlorobis(dimethyl sulfoxide)(imidazole)-ruthenium(III) (mer-$RuCl_3(DMSO)_2(Im)$) (**6b**)*

A 0.5 g amount of **2** (1.1 mmol) was dissolved in 8 ml of CH_2Cl_2 and 0.28 g of imidazole (4 mmol) was added. In a few minutes at r.t. the solution turned from red to brown–yellow. Addition of a few drops of diethyl ether caused the precipitation of the microcrystalline product. After 30 min it was filtered off, washed with cold CH_2Cl_2 and diethyl ether, and vacuum dried at r.t. (yield 70%). *Anal.* Calc. for $RuCl_3(DMSO)_2(Im)$ (M_r = 431.76): C, 19.47; H, 3.73; N, 6.48. Found: C, 19.40; H, 3.90; N, 6.65%.

Crystal data

Crystals were grown from DMSO/acetone (1:5) solutions upon addition of diethyl ether.

Crystallization of the imidazole derivative **5b** caused the substitution of the two DMSO molecules with one molecule of water and one of acetone. Water very likely comes from DMSO, as this solvent was not dried for synthetic purposes.

TABLE 1. Crystallographic data for **5a**, **5b** and **6a**

	5a	**5b**	**6a**
Formula	$C_6H_{21}Cl_4NNaO_3S_3Ru$	$C_8H_{18}Cl_4N_2NaO_3S$	$RuC_4H_{15}Cl_3NO_2S_2Ru$
Molecular weight	517.3	488.2	380.7
Crystal system	triclinic	triclinic	monoclinic
Space group	$P\bar{1}$	$P\bar{1}$	$P2_1/n$
a (Å)	9.578(4)	10.790(5)	10.110(4)
b (Å)	12.480(4)	11.411(5)	9.718(6)
c (Å)	9.594(3)	7.658(4)	14.101(5)
α (°)	104.33(2)	105.92(4)	90
β (°)	119.04(3)	93.61(4)	108.89(3)
γ (°)	80.71(3)	83.50(3)	90
V (Å^3)	970.3(7)	900.4(8)	1311(1)
Z	2	2	4
D_{calc} (g cm^{-3})	1.771	1.802	1.929
μ (Mo Kα) (cm^{-1})	16.8	15.94	20.73
λ (Å)		0.71069 (graphite-monochromated Mo Kα)	
Scan type	$\omega/2\theta$	$\omega/2\theta$	$\omega/2\theta$
θ Range (°)	3–30	3–30	3–30
Intensity monitors[a]	3	3	3
Unique data with $I>3\sigma(I)$	4897	4932	3152
No. variables	190	181	118
Residuals in final Difference map (e Å^{-3})	+0.89, −1.50	+0.93, −0.75	+0.46, −0.47
R[b]	0.039	0.031	0.022
R_w[c]	0.065	0.032	0.023
w	$[1+\sigma^2(F_o)+0.04F_o^2]^{-1}$	1	1
GOF[d]	2.33	0.811	1.000

[a]Measured after each 4000 s. [b]$R=\Sigma\|\|F_o\|-|F_c\|\|/\Sigma|F_o|$. [c]$R_w=[\Sigma w(|F_o|-|F_c|)^2/\Sigma w|F_o|^2]^{1/2}$. [d]$GOF=[\Sigma w(|F_o|-|F_c|)^2/(m-n)]^{1/2}$; m = no. of observations, n = no. of variables.

Unit cell parameters of the three compounds were obtained by least-squares methods from the setting angles of 25 accurately centred reflections on an Enraf-Nonius CAD4 diffractometer. A summary of the crystal data, data collection and refinement is given in Table 1. Intensities were corrected for Lorentz–polarization factors and an empirical absorption correction was also applied, by using ψ scan data. No correction for extinction was applied.

Structure determination and refinement

The structures were solved by the heavy atom method through Patterson and Fourier syntheses. In **5a**, one of the two crystallization DMSO molecules was found to be disordered, in such a way that the oxygen atom (O3) and one methyl group (C5) are fixed, while the sulfur atom and the other methyl group occupy two close positions, S3, S4, and C6, C7, with half occupancy factors. All hydrogen atoms were included at calculated positions, except those of C6 and C7. Hydrogen atom parameters were held fixed during refinement with isotropic thermal factors $B=1.3B_{eq}$ of the atom to which they are bonded. Neutral atom scattering factors and anomalous dispersion terms were taken from the literature [20]. All calculations were done by using the Enraf-Nonius SDP programs [21] on a PDP 11/44 computer.

The final positional parameters for non-hydrogen atoms of **5a**, **5b** and **6a** are listed in Tables 2, 3 and 4, respectively. See also 'Supplementary material'.

Results and discussion

Dimethyl sulfoxide derivatives

As already reported in previous papers [8, 10], the chemical behaviour of the Ru(III)–sulfoxide precursors in solution is characterized by the rather facile dissociation of one of the two *trans* S-bonded sulfoxides. Accordingly, we found that both **1Na** and **2**, in organic solvent solution and at room temperature, can rapidly react with a slight excess of nitrogen ligand replacing one DMSO as schematically reported in Fig. 1.

The anionic compounds **5** usually have two DMSO molecules of crystallization and are therefore better formulated as Na[*trans*-$RuCl_4$(DMSO)(L)]·2DMSO. As shown by spectroscopic data, acetone (used as reaction medium) and, more seldom, water molecules can sometimes partially replace the DMSO of crystallization, affecting the reproducibility of the elemental analysis of different preparations. Compounds with

TABLE 2. Atomic parameters[a] of Na[*trans*-$RuCl_4$-(DMSO)(NH_3)]·2DMSO (**5a**) with e.s.d.s in parentheses

Atom	x	y	z	B (Å^2)
Ru	−0.00716(3)	0.26306(2)	0.38743(2)	2.215(4)
Cl1	0.0802(1)	0.14797(7)	0.5761(1)	3.64(2)
Cl2	−0.0754(1)	0.38462(7)	0.2092(1)	3.71(2)
Cl3	−0.1777(1)	0.36444(8)	0.4891(1)	3.73(2)
Cl4	0.1736(1)	0.16639(9)	0.2938(1)	4.08(2)
S1	−0.21347(9)	0.15308(6)	0.20310(9)	2.64(2)
S2	−0.4193(1)	0.1992(1)	−0.3676(1)	3.81(2)
S3	−0.7382(2)	0.4317(2)	0.0795(2)	3.63(3)
S4	−0.6596(3)	0.3589(2)	0.0927(3)	6.40(5)
Na	−0.3958(2)	0.3747(1)	−0.0097(2)	3.72(4)
O1	−0.3408(3)	0.1994(2)	0.0634(3)	3.84(7)
O2	−0.4688(3)	0.3060(3)	−0.2848(3)	4.10(7)
O3	−0.6148(3)	0.4413(3)	0.0242(3)	4.65(6)
N	0.1738(3)	0.3710(3)	0.5621(3)	3.12(6)
C1	−0.3106(4)	0.1085(4)	0.2948(5)	4.15(8)
C2	−0.1522(5)	0.0216(3)	0.1201(5)	4.2(1)
C3	−0.4819(5)	0.0927(4)	−0.3199(5)	4.5(1)
C4	−0.2087(5)	0.1802(6)	−0.2464(6)	5.9(1)
C5	−0.6327(8)	0.4278(7)	0.2832(6)	7.4(2)
C6	−0.769(1)	0.2821(9)	0.006(1)	6.8(3)
C7	−0.864(1)	0.354(1)	−0.028(1)	7.3(3)

[a]Anisotropically refined atoms are given in the form of equivalent thermal parameters defined as: $4/3[a^2\beta_{11}+b^2\beta_{22}+c^2\beta_{33}+ab(\cos\gamma)\beta_{12}+ac(\cos\beta)\beta_{13}+bc(\cos\alpha)\beta_{23}]$.

TABLE 3. Atomic parameters[a] of Na[*trans*-$RuCl_4$-(DMSO)(Im)]·H_2O,Me_2CO (**5b**) with e.s.d.s in parentheses

Atom	x	y	z	B (Å^2)
Ru	0.21248(2)	0.20315(2)	0.02184(2)	2.098(3)
Cl1	0.18812(9)	0.32737(7)	−0.17806(9)	3.92(2)
Cl2	0.42545(7)	0.2217(1)	0.0523(1)	5.02(2)
Cl3	0.2361(1)	0.08059(7)	0.2270(1)	4.63(2)
Cl4	−0.00398(7)	0.19431(9)	0.0114(1)	4.35(2)
S	0.23664(6)	0.03793(6)	−0.22865(8)	2.33(1)
Na	0.0884(1)	−0.1018(1)	−0.6580(2)	3.88(3)
O1	0.1295(2)	0.0237(2)	−0.3622(3)	3.19(4)
O2	0.2762(2)	−0.2275(2)	−0.6702(4)	5.02(6)
O3	0.0002(2)	−0.2235(2)	−0.4800(4)	4.44(5)
N1	0.1867(2)	0.3587(2)	0.2396(3)	2.87(4)
N2	0.2090(4)	0.4959(3)	0.5031(5)	6.8(1)
C1	0.3705(3)	0.0388(3)	−0.3525(4)	3.91(7)
C2	0.2722(3)	−0.1049(3)	−0.1778(4)	3.88(7)
C3	0.1071(3)	0.4562(3)	0.2468(4)	3.61(6)
C4	0.1188(3)	0.5407(3)	0.4047(4)	3.27(6)
C5	0.2522(4)	0.3816(3)	0.4031(4)	4.17(7)
C6	0.3176(4)	−0.3794(4)	−0.9463(6)	5.9(1)
C7	0.3451(3)	−0.3123(3)	−0.7542(5)	4.09(7)
C8	0.4615(4)	−0.3564(5)	−0.6660(7)	6.8(1)

[a]Anisotropically refined atoms are given in the form of equivalent thermal parameters defined as: $4/3[a^2\beta_{11}+b^2\beta_{22}+c^2\beta_{33}+ab(\cos\gamma)\beta_{12}+ac(\cos\beta)\beta_{13}+bc(\cos\alpha)\beta_{23}]$.

L = NH_3 (**5a**), imidazole (Im, **5b**), *N*-methylimidazole (MeIm), pyrazole (Pz), indazole (Ind), pyridine (Py), isoquinoline (Iq) have been synthesized and characterized up to now, but other derivatives might be easily synthesized with similar procedures.

TABLE 4. Atomic parameters[a] of *mer,cis*-$RuCl_3(DMSO)_2(NH_3)$ (**6a**) with e.s.d.s in parentheses

Atom	x	y	z	B (Å^2)
Ru	0.09938(2)	0.16475(2)	0.37074(1)	1.781(3)
Cl1	0.33294(6)	0.17718(8)	0.38125(5)	2.96(1)
Cl2	0.08621(7)	0.40133(7)	0.39429(5)	3.01(1)
Cl3	0.09238(7)	−0.07646(7)	0.35864(5)	2.96(1)
S1	−0.21749(6)	0.25391(7)	0.31972(5)	2.51(1)
S2	0.02918(6)	0.18153(7)	0.20100(4)	2.10(1)
O1	−0.1025(2)	0.1505(2)	0.3758(1)	2.39(3)
O2	−0.1217(2)	0.1557(2)	0.1515(1)	3.13(4)
N	0.1570(2)	0.1442(3)	0.5276(2)	2.90(5)
C1	−0.3627(3)	0.1448(4)	0.2652(3)	4.71(9)
C2	−0.2678(4)	0.3289(4)	0.4174(3)	5.18(8)
C3	0.0699(3)	0.3420(3)	0.1579(2)	3.38(6)
C4	0.1225(3)	0.0701(4)	0.1453(2)	3.66(6)

[a]Anisotropically refined atoms are given in the form of equivalent thermal parameters defined as; $4/3[a^2\beta_{11}+b^2\beta_{22}+c^2\beta_{33}+ab(\cos\gamma)\beta_{12}+ac(\cos\beta)\beta_{13}+bc(\cos\alpha)\beta_{23}]$.

All the anionic derivatives are highly water soluble. The solubility of the neutral complexes **6** is less pronounced and strongly dependent on the nature of the nitrogen ligand.

The anionic and neutral derivatives have been characterized mainly by means of solid state IR and ^{1}H NMR in D_2O. However, owing to the paramagnetism of the Ru(III) nucleus and to the almost total absence of previous reports on this subject, a complete assignment of the NMR spectra was not attempted.

IR band assignment was performed according to current literature data [5, 8, 12, 22–27] and was supported by the systematic analysis of the corresponding compounds with DMSO-d_6. All the complexes belonging to each class have some features in common. In fact, every anionic complex **5** is characterized by a strong band at about 1090 cm^{-1}, that is not shifted upon deuteration and can be safely attributed to the S–O stretching mode of DMSO. This absorption is always accompanied by a Ru–S stretching band at about 430 cm^{-1}. Other common features are the S–O stretching band of the DMSO molecules of crystallization at about 1020 cm^{-1} and the strong Ru–Cl stretching band (sometimes splitted) approximately at 340 cm^{-1}. On the other hand, the spectra of the neutral derivatives **6** clearly show the presence of two differently bonded dimethyl sulfoxides, one through the sulfur atom (ν(S–O) at about 1090 cm^{-1} and ν(Ru–S) around 420 cm^{-1}) and the other through the oxygen atom (ν(S–O) at about 910 cm^{-1} and ν(Ru–O) around 495 cm^{-1}). As in the precursor **2**, only a single strong Ru–Cl stretching band with an enlarged shape is observed in every case at about 330 cm^{-1}. In this paper we report in detail the spectroscopic results concerning the ammonia (**5a** and

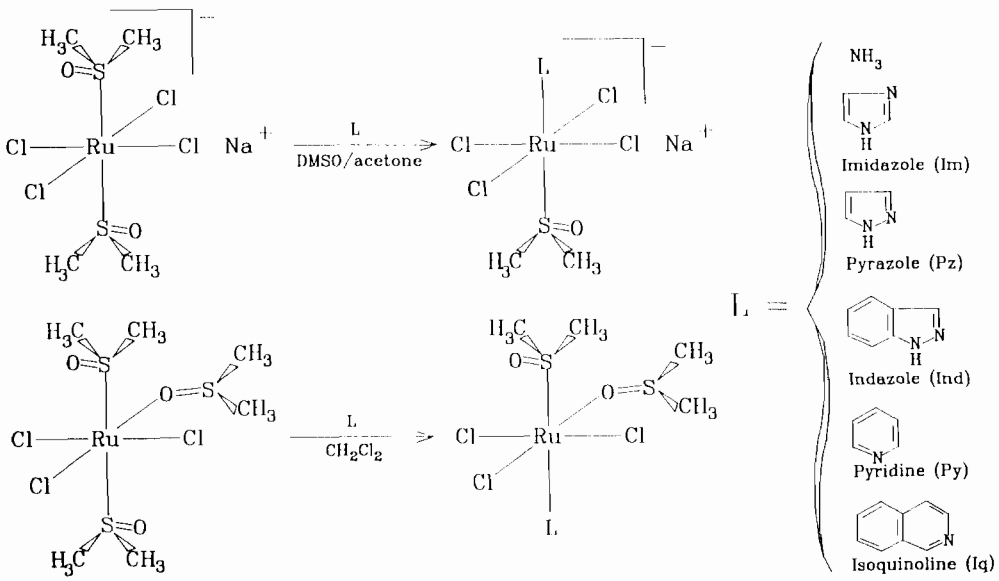

Fig. 1. Scheme of the synthetic path to the anionic (**5**) and neutral (**6**) Ru(III) derivatives.

6a, Table 5) and imidazole (**5b** and **6b**, Table 6) derivatives. In the case of the ammonia complexes, the almost total absence of ligand absorption bands allowed a more detailed band assignment.

The D_2O ^1H NMR spectra of the anionic complexes **5** share the common feature of a broad signal centered at about -15 ppm. This peak, that could be unambiguously attributed to the protons of S-bonded DMSO by comparison with the DMSO-d_6 derivatives, is shifted approximately 2 ppm downfield compared to the precursor [8]. Analysis of the neutral complexes was limited to the ammonia and imidazole derivatives, due to solubility limits. Similarly to the precursor [8], they both have a broad band around -14.5 ppm (S-bonded DMSO) and a slightly sharper band of equal intensity around 10.7 ppm (O-bonded DMSO).

Owing to their lower intensity, detection of the nitrogen ligand signals was sometimes difficult, in particular with the slightly soluble neutral derivatives. As an example we report the D_2O spectrum of Na[*trans*-$RuCl_4$(DMSO)(Im)]·2DMSO (**5b**) (Fig. 2). Beside the DMSO protons signal (and the signal of free DMSO at 2.72 ppm, not shown in the Figure), the spectrum of the complex shows three signals of equal intensity for the coordinated imidazole, two very broad peaks centered at -7.8 and -5.6 ppm and a sharper resonance at -3.5 ppm. No free imidazole was detected in freshly prepared solutions. As in the case of $[Ru(NH_3)_5(Im)]^{3+}$ [28], the narrowest peak can be safely attributed to H5, which is further removed from the paramagnetic center, while the two other originate from H2 and H4. The imidazole resonances are quite different from those observed in the similar complex (ImH)[*trans*-$RuCl_4(Im)_2$]. In a freshly prepared solution of **ICR**, in fact, the three signals for the two equivalent imidazole ligands are found at -6.0 ppm (H5) and at -16.1 and -21.5 ppm (H2 and H4).

As a general remark, the NMR spectra of complexes **5** and **6** clearly showed that neither DMSO or the nitrogen ligand are readily replaced in aqueous solution.

Both the IR and the NMR spectra strongly suggested that the disposition of the other ligands in **1Na** and **2** was left unaltered by the replacement of a DMSO with a nitrogen ligand. This hypothesis was further supported by the UV–Vis absorption spectra. In fact, both anionic and neutral derivatives have electronic absorption spectra very similar to that of the corresponding precursor (Table 7). Interestingly, each nitrogen ligand induces a similar shift of the main absorption maximum in both classes of compounds.

The single-crystal X-ray analysis of some anionic (**5a**, **5b**) and neutral (**6a**) derivatives definitively confirmed the structures proposed for the two classes of compounds (see below).

Molecular structures

The molecular structures of Na[*trans*-$RuCl_4$(DMSO)(NH_3)]·2DMSO (**5a**), Na[*trans*-$RuCl_4$(DMSO)(Im)]·H_2O,Me_2CO (**5b**) and *mer*,*cis*-$RuCl_3$(DMSO)(DMSO)(NH_3) (**6a**) are depicted in Figs. 3, 4, and 5, respectively. Bond lengths and angles are given in Tables 8, 9 and 10, respectively.

In both ruthenates, **5a** and **5b**, the metal atom has the expected distorted octahedral geometry, with four chlorine atoms in the equatorial positions and a DMSO *trans* to the N-ligand. In **5a**, the sodium ion is bound to the oxygen atom, O1, of the coordinated DMSO and to the oxygen atoms, O2 and O3, of the two

TABLE 5. Vibrational frequencies (cm^{-1}) for the main absorption bands of Na[*trans*-$RuCl_4(DMSO)(NH_3)$]·2DMSO (**5a**), *mer,cis*-$RuCl_3(DMSO)_2(NH_3)$ (**6a**), and their hexadeuterated analogues **5a**(DMSO-d_6) and **6a**(DMSO-d_6) between 4000 and 300 cm^{-1}

Frequency (cm^{-1})				
5a	**5a**(DMSO-d_6)	**6a**	**6a**(DMSO-d_6)	Assignment
3300s[a]	3303s	3312s	3310s	
3244m	3245m	3243m	3241m	νN–H[b]
3173m	3171m	3171m	3170m	
2997m	2253m (1.33)[c]	3001m	2253m (1.33)	νC–H
2918m	2130m (1.37)	2918m	2128w (1.37)	
1611s	1616s	1614s	1616s	δ_d(NH)
1439m	1032m (1.39)	1426m	1030sh (1.39)	
1405s	1011s (1.39)	1404s	1007s (1.39)	δ_d(CH)
1309m	1003m (1.30)	1307s		
		1295m	950sh (1.36)	
		1281m		
1282s	1283s	1248s	1247s	δ_s(NH)
1088vs	1092vs	1088vs	1093vs	νS–O (DMSO)
1025vs	[d]			νS–O (crystallization)
979w	828s	1031m	823s	
961s	822s	1018s	765m	ρ(CH)
938m	770m	982s		
907w		962w		
		910vs	907vs	νS–O (DMSO)
709s	700w (1.01)	724m	692w (1.05)	
687m	635w (1.08)	690m	633w (1.09)	νC–S
		498s	472s (1.05)	νRu–O
460w	457w	455w	[d]	νRu–N
427m	396m (1.08)	419m	384m (1.09)	νRu–S
395m	[d]	375m	[d]	δC–S–O
338vs				
319vs	317vs	329vs	322vs	νRu–Cl

[a]sh, shoulder; w, weak; m, medium; s, strong; vs, very strong; br, broad. [b]ν, stretching; δ, deformation; ρ, rocking. [c]Numbers in parentheses refer to the isotope ratios. [d]Peak hidden by other absorptions.

crystallization DMSO molecules. An extremely distorted tetrahedral environment of Na^+ is achieved through further coordination to the oxygen atom, O3′, of the symmetry related molecule at $-1-x,1-y,-z$. In **5b**, the sodium ion has again a highly distorted tetrahedral geometry, being coordinated to the oxygen atoms of the crystallization acetone (O2) and water (O3) molecules, and to the oxygen atoms of the Ru-bonded DMSO (O1) and its symmetry analogue (O1′) of the molecule at $-x,-y,-1-z$.

In **6a** the three chlorine atoms occupy the meridianal positions, with a DMSO *trans* to NH_3 and a DMSO *trans* to Cl. The Ru–O bond length is very close to that found in **2** (2.077(3) Å) [8].

The average values of the Ru–Cl bond lengths are well comparable in the three compounds (2.348(7) Å in **5a**, 2.34(2) Å in **5b**, and 2.34(1) Å in **6a**) and close to the average value of 2.350(7) Å found in related Ru(III) complexes [9]. As expected [8–10] these distances are *c*. 0.06 Å shorter than those found in the *trans* Cl–Ru(II)–Cl group (av. 2.41(1) Å).

Similarly, the Ru(III)–NH_3 distances in **5a** and **6a** are shorter than the average value of 2.150(7) Å, found for the Ru(II)–NH_3 distance in *cis,fac*-$RuCl_2(DMSO)_3NH_3$ and *trans,cis,cis*-$RuCl_2(DMSO)_2(NH_3)_2\cdot H_2O$ [14]. It is interesting to observe that a similar shortening of 0.040 Å of the Ru–NH_3 bond length has been already observed when $[Ru(NH_3)_6]I_2$ (2.144(4) Å) was compared to $[Ru(NH_3)_6][BF_4]_3$ (2.104(4) Å) [29].

TABLE 6. Vibrational frequencies (cm^{-1}) for the main absorption bands of Na[*trans*-$RuCl_4$(DMSO)(Im)]·2DMSO (**5b**), *mer,cis*-$RuCl_3$(DMSO)$_2$(Im) (**6b**), and their hexadeuterated analogues **5b**(DMSO-d_6) and **6b**(DMSO-d_6) between 1600 and 300 cm^{-1}

Frequency (cm^{-1})				
5b	**5b**(DMSO-d_6)	**6b**	**6b**(DMSO-d_6)	Assignment
1413m[a]	1046m (1.35)[b]	1412m	1028m (1.37)	δ(CH)[c]
1310m	999m (1.31)	1311m	1011m (1.30)	
1096s	1099s	1093s	1096s	νS–O (DM*S*O)
1020s	1026s			νS–O (crystallization)
1007s	820sh	1020s	825s	
959w	785m	976m	771m	ρ(CH)
951m	770m		749m	
941w				
		902s	902s	νS–O (DMS*O*)
731w		728m	704w (1.03)	νC–S
690w	636w (1.08)	687m		
		496s	472s (1.05)	νRu–O
428m	396m (1.08)	422m	390m (1.08)	νRu–S
398m	379w			δC–S–O
345s	339s		341s	νRu–Cl
325s	322s	335s	326s	
Imidazole characteristic absorptions				
1060s, 840m, 827m, 660s, 618m				

[a]sh, shoulder; w, weak; m, medium; s, strong; vs, very strong; br, broad. [b]Numbers in parentheses refer to the isotope ratios. [c]ν, stretching; δ, deformation; ρ, rocking.

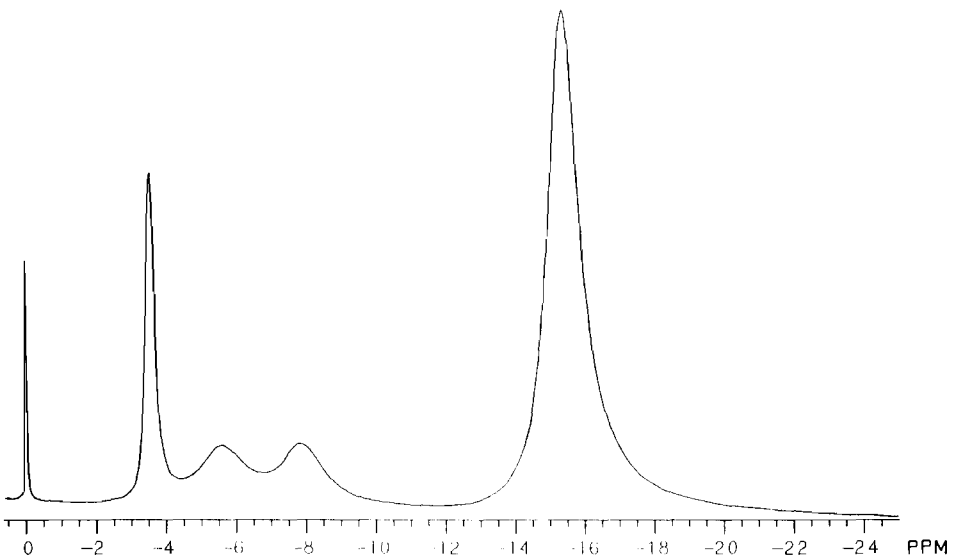

Fig. 2. ^{1}H NMR spectrum, (360 MHz, D_2O) of Na[*trans*-$RuCl_4$(DM*S*O)Im] (**5b**).

This has been attributed to the increase of the metal positive charge [29].

The Ru(III)–N(Im) bond distance in **5b** is similar to that of 2.079(3) Å found in [(Im)H][*trans*-$RuCl_4Im_2$] [16a]. These values are slightly shorter than those of the ammonia derivatives, as expected from the change of hybridization of the nitrogen atoms, from sp^3 to sp^2.

TABLE 7. UV–Vis absorption bands and half-wave potentials of anionic and neutral complexes in aqueous solution

Compound	λ_{max} (nm)	(ϵ (M^{-1} cm^{-1}))	$E_{1/2}$ (V)
Na[*trans*-$RuCl_4(DMSO)(H_2O)$]	464 (592)	395 (5212)	0.107[a]
Na[*trans*-$RuCl_4(DMSO)(NH_3)$]	449 (449)	385 (3684)	0.029
Na[*trans*-$RuCl_4$(DMSO)(Im)]	451 (488)	390 (3644)	−0.001
Na[*trans*-$RuCl_4$(TMSO)(Im)]	451 (496)	388 (3411)	
Na[*trans*-$RuCl_4$(DMSO)(MeIm)]	451 (535)	389 (3880)	0.005
Na[*trans*-$RuCl_4$(DMSO)(Pz)]	456 (673)	389 (4776)	0.065
Na[*trans*-$RuCl_4$(DMSO)(Ind)]	461 (648)	395 (4357)	0.089
Na[*trans*-$RuCl_4$(TMSO)(Ind)]	461 (492)	395 (3261)	
Na[*trans*-$RuCl_4$(DMSO)(Py)]	458 (438)	394 (3568)	0.065
Na[*trans*-$RuCl_4$(TMSO)(Py)]	457 (474)	394 (3539)	0.062
Na[*trans*-$RuCl_4$(DMSO)(Iq)]	458 (488)	395 (3850)	0.066
Na[*trans*-$RuCl_4$(TMSO)(Iq)]	457 (492)	395 (3497)	
mer-$RuCl_3(DMSO)_2(H_2O)$	426 (1060)	364 (3260)	0.186[a]
mer-$RuCl_3(DMSO)_2(NH_3)$	414 (1174)	355 (3222)	0.117
mer-$RuCl_3(DMSO)_2$(Im)	413 (1034)	358 (2529)	0.101
mer-$RuCl_3(TMSO)_2$(Im)[b]	413	358	

[a]See ref. 15. [b]ϵ not evaluated due to the low solubility of the complex.

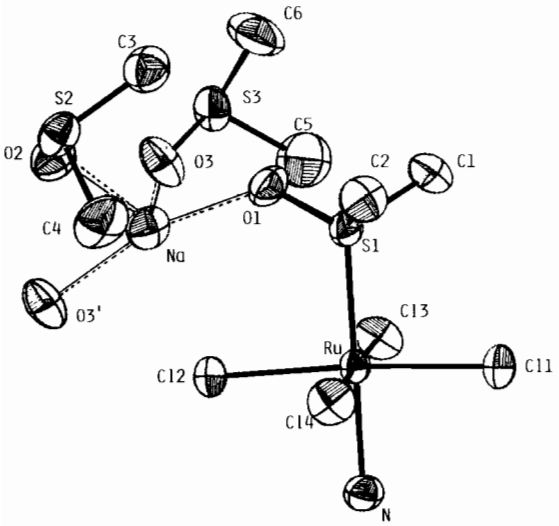

Fig. 3. ORTEP drawing of Na[*trans*-$RuCl_4(DMSO)(NH_3)$]·2DMSO (**5a**) showing the atom numbering scheme (thermal ellipsoids at 50% probability level). O3′ refers to the oxygen atom of a DMSO symmetry equivalent molecule at $-1-x$, $1-y$, $-z$, not shown for sake of clarity.

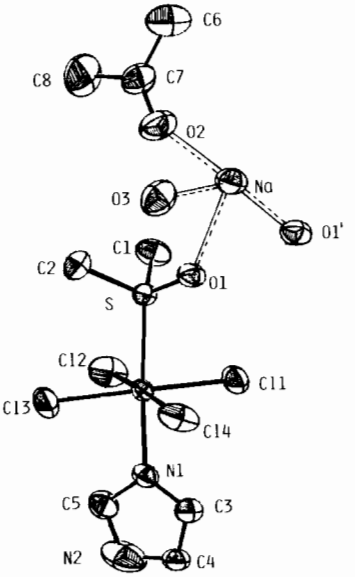

Fig. 4. ORTEP drawing of Na[*trans*-$RuCl_4(DMSO)(Im)]\cdot H_2O$, Me_2CO (**5b**) showing the atom numbering scheme (thermal ellipsoids at 50% probability level). O1′ refers to the oxygen atom of a DMSO symmetry equivalent molecule at $-x$, $-y$, $-1-z$, not shown for sake of clarity.

On the other hand, the Ru–S bond distances in **5a**, **5b** and **6a** are significantly shorter than the average value of 2.34(1) Å found for the Ru(III)–S, *trans* to S, in the precursors [6, 8–10]. It is also interesting to observe that the above Ru–S bond distances do not show any appreciable reduction with respect to the equivalent Ru(II)–S distance of 2.2877(5) Å in *cis,fac*-$RuCl_2(DMSO)_3NH_3$ [16]. Moreover, they are longer than the Ru(II)–S bond distances in *trans,cis,cis*-$RuCl_2(DMSO)_2(NH_3)_2\cdot H_2O$ (2.2350(6) and 2.2468(6) Å), and in $[Ru(NH_3)_5(DMSO)]^{2+}$ (2.188(3) Å) [30].

The dependence of the Ru–S bond length on the ruthenium oxidation state and on the nature of the ligand in *trans* might be rationalized in terms of π backbonding contribution in the Ru–DMSO bond. This, in fact, should increase from Ru(III) to Ru(II) and with the number of σ-donor ligands because of the increased negative charge density on the metal center, and decrease with the number of π accepting ligands, such as two *trans* DMSOs. Furthermore, an increase of the π bond character of the Ru–S bond is expected to reduce the positive charge on the sulfur atom [26] and hence also the p_π–d_π overlap between O and S orbitals.

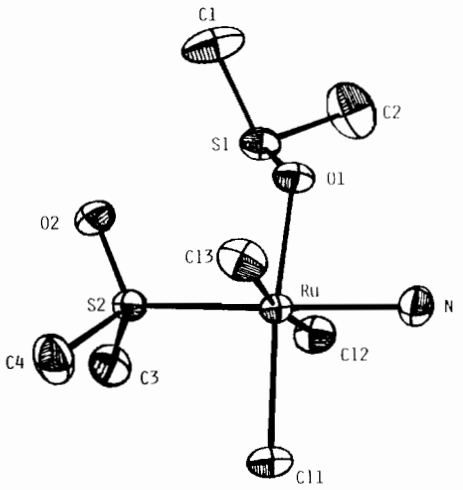

Fig. 5. ORTEP drawing of *mer,cis*-$RuCl_3(DMSO)_2(NH_3)$ (**6a**) showing the atom numbering scheme (thermal ellipsoids at 50% probability level).

The shortening of the Ru–S bond length in these complexes compared to the precursors might therefore be interpreted with an increased π backbonding contribution from Ru(III). This bonding scheme is supported by the trend of the S–O bond lengths. In fact, the average S–O bond distance of 1.466(5) Å in [*trans*-$RuCl_4(DMSO)_2]^-$ is shorter than that of 1.482(5) Å in **5a**, **5b** and **6a**. This trend is also reflected in the S–O stretching frequency that, for example, decreases from 1115 cm^{-1} in **1** to approx. 1090 cm^{-1} in **5a** and **6a** (Table 6).

It is interesting to note that the S–O bond distances in the DMSO molecules of crystallization bound to Na^+ in **5a** are markedly longer than those in the Ru-coordinated molecules. The average bond distance of 1.53(2) Å is in the range of values found for other alkaly metal–DMSO complexes, e.g. 1.54(2) Å [31], 1.50(2) Å [32], as well as for protonated $[(DMSO)_2H]^+$ cations, e.g. 1.544(6) Å [33], 1.534(3) Å [34], 1.532(4) Å [8]. Longer distances are found in $[(DMSO)H]^+$ (1.585(8) Å) [35] and in $[(TMSO)H]^+$ (1.589(3) Å) [10]. All these values are greater than the S–O bond length in free DMSO. Unfortunately, the available X-ray data for free DMSO are of low accuracy and strongly dependent on the experimental temperature [26]. Probably, the most accurate S–O bond distance for free DMSO is that of 1.485(6) Å, obtained by gas-phase microwave spectroscopy on various isotopically substituted species [36]. As a matter of fact, this value is comparable to those found in some solvates, e.g. 1.488(5) Å [37], 1.49(1) Å [38]. 1.494(4) Å [39].

Tetramethylene sulfoxide derivatives

Anionic and neutral derivatives of general formula Na[*trans*-$RuCl_4(TMSO)(L)]\cdot TMSO$ (**7**) and *mer*-$RuCl_3(TMSO)_2(L)$ (**8**) could be obtained from **3Na** and **4**, respectively, by adopting synthetic procedures very similar to those already reported for the corresponding DMSO compounds **5** and **6**. Even though in this case no X-ray determination was performed, the IR and UV–Vis spectroscopic data allowed the unambiguous structural characterization of the complexes.

IR spectroscopy confirmed the presence of exclusively S-bonded TMSO in the anionic derivatives **7** (ν(S–O) at about 1105 cm^{-1}) and of both S-bonded and O-bonded TMSO in the neutral ones (**8**) (ν(S–O) at about 1105 and 910 cm^{-1}, respectively). Moreover, both anionic and neutral compounds have electronic absorption spectra almost superimposable to those of the corresponding DMSO derivatives. Some examples are reported in Table 7.

Electrochemistry

The cyclic voltammetry of the complexes **5–8** in aqueous solution at a scan rate of 1 V/s, reveals in

TABLE 8. Bond distances (Å) and angles (°) for Na[*trans*-$RuCl_4(DMSO)(NH_3)]\cdot 2DMSO$ (**5a**)

Distances			
Ru–Cl1	2.339(2)	S1–O1	1.479(3)
Ru–Cl2	2.352(2)	S1–C1	1.776(6)
Ru–Cl3	2.344(2)	S1–C2	1.780(4)
Ru–Cl4	2.358(1)	S2–O2	1.508(3)
Ru–S1	2.2797(7)	S2–C3	1.777(7)
Ru–N	2.108(3)	S2–C4	1.784(4)
Na–O1	2.363(3)	S3–O3	1.542(4)
Na–O2	2.338(3)	S3–C5	1.720(6)
Na–O3	2.272(4)	S3–C6	1.84(2)
Na–O3′	2.356(4)	S4–O3	1.558(5)
S1–C1	1.784(2)	S4–C5	1.727(7)
		S4–C7	1.726(9)
Angles			
Cl1–Ru–Cl2	175.58(2)	Ru–S1–O1	117.1(1)
Cl1–Ru–Cl3	90.51(4)	Ru–S1–C1	112.2(1)
Cl1–Ru–Cl4	89.44(4)	Ru–S1–C2	113.9(1)
Cl1–Ru–S1	91.82(3)	O1–S1–C1	106.3(2)
Cl1–Ru–N	88.6(1)	O1–S1–C2	106.3(2)
Cl2–Ru–Cl3	90.95(4)	C1–S1–C2	99.1(2)
Cl2–Ru–Cl4	88.92(5)	O2–S2–C3	105.2(2)
Cl2–Ru–S1	92.39(4)	O2–S2–C4	106.1(2)
Cl2–Ru–N	87.3(1)	C3–S2–C4	98.6(3)
Cl3–Ru–Cl4	177.46(4)	O3–S3–C5	106.7(3)
Cl3–Ru–S1	88.46(3)	O3–S3–C6	99.2(5)
Cl3–Ru–N	88.1(1)	C5–S3–C6	96.7(4)
Cl4–Ru–S1	94.10(3)	O3–S4–C5	105.8(3)
Cl4–Ru–N	89.4(1)	O3–S4–C7	102.5(5)
S1–Ru–N	176.52(9)	C5–S4–C7	105.3(5)
O1–Na–O2	95.6(1)		
O1–Na–O3	103.1(1)		
O1–Na–O3′	165.2(1)		
O2–Na–O3	110.6(2)		
O2–Na–O3′	94.1(1)		
O3–Na–O3′	83.9(1)		

O3′ is referred to O3 by the symmetry operation $-1-x, 1-y, -z$.

TABLE 9. Bond distances (Å) and angles (°) for Na[*trans*-$RuCl_4(DMSO)(Im)]\cdot H_2O,Me_2CO$ (**5b**)

Distances			
Ru–Cl1	2.3403(9)	S–O1	1.487(2)
Ru–Cl2	2.3227(8)	S–C1	1.779(3)
Ru–Cl3	2.3588(9)	S–C2	1.773(3)
Ru–Cl4	2.3447(8)	O2–C7	1.207(4)
Ru–S	2.2956(6)	N1–C3	1.317(4)
Ru–N1	2.081(2)	N1–C5	1.373(4)
Na–O1	2.370(2)	N2–C4	1.334(5)
Na–O1′	2.418(2)	N2–C5	1.365(5)
Na–O2	2.337(3)	C3–C4	1.333(4)
Na–O3	2.489(3)	C6–C7	1.490(5)
		C7–C8	1.492(6)
Angles			
Cl1–Ru–Cl2	90.80(4)	Ru–S–O1	115.53(8)
Cl1–Ru–Cl3	179.12(2)	Ru–S–C1	112.7(1)
Cl1–Ru–Cl4	90.17(4)	Ru–S–C2	114.4(9)
Cl1–Ru–S	87.43(2)	O1–S–C1	106.3(1)
Cl1–Ru–N1	89.55(7)	O1–S–C2	106.7(1)
Cl2–Ru–Cl3	89.32(5)	C1–S–C2	99.8(2)
Cl2–Ru–Cl4	175.95(3)	C3–N1–C5	106.2(2)
Cl2–Ru–S	92.43(3)	C4–N2–C5	107.9(3)
Cl2–Ru–N1	88.41(8)	N1–C3–C4	111.2(3)
Cl3–Ru–Cl4	89.65(4)	N2–C4–C3	107.4(3)
Cl3–Ru–S	93.44(3)	N1–C5–N2	107.4(4)
Cl3–Ru–N1	89.58(7)	O2–C7–C6	122.5(3)
Cl4–Ru–S	91.54(3)	O2–C7–C8	120.6(3)
Cl4–Ru–N1	87.66(8)	C6–C7–C8	116.9(3)
S–Ru–N1	176.88(7)	Ru–N1–C3	127.1(2)
		Ru–N1–C5	127.7(2)
O1–Na–O1′	90.35(7)		
O1–Na–O2	94.84(9)		
O1–Na–O3	81.41(9)		
O1′–Na–O2	163.6(1)		
O1′–Na–O3	76.33(9)		
O2–Na–O3	89.1(2)		

O1′ is referred to O1 by the symmetry operation $-x, -y, -1-z$.

TABLE 10. Bond distances (Å) and angles (°) for *mer,cis*-$RuCl_3(DMSO)_2(NH_3)$ (**6a**)

Distances			
Ru–Cl1	2.3207(7)	S1–O1	1.547(2)
Ru–Cl2	2.3330(8)	S1–C1	1.773(3)
Ru–Cl3	2.3497(7)	S1–C2	1.773(4)
		S2–O2	1.479(2)
Ru–S2	2.2714(6)	S2–C3	1.770(3)
Ru–O1	2.070(2)	S2–C4	1.777(4)
Ru–N	2.107(2)		
Angles			
Cl1–Ru–Cl2	92.49(3)	O1–S1–C1	102.3(1)
Cl1–Ru–Cl3	93.59(3)	O1–S1–C2	103.1(1)
Cl1–Ru–S2	91.60(2)	C1–S1–C2	100.2(2)
Cl1–Ru–O1	174.60(5)	Ru–S2–O2	114.08(9)
Cl1–Ru–N	90.48(7)	Ru–S2–C3	113.41(9)
Cl2–Ru–Cl3	172.62(4)	Ru–S2–C4	113.10(9)
Cl2–Ru–S2	93.81(2)	O2–S2–C3	107.8(1)
Cl2–Ru–O1	87.63(6)	O2–S2–C4	107.6(1)
Cl2–Ru–N	87.30(7)	C3–S2–C4	99.8(1)
Cl3–Ru–S2	90.20(2)	Ru–O1–S1	121.7(1)
Cl3–Ru–O1	85.93(6)		
Cl3–Ru–N	88.48(7)		
S2–Ru–O1	93.78(5)		
S2–Ru–N	177.60(7)		
O1–Ru–N	84.14(8)		

every case a reversible to quasi-reversible Ru(III)/Ru(II) electron transfer, with peak to peak separations in the range 60–72 mV. Complete stability of the reduced forms on this time scale is deduced from the observed anodic to cathodic peak current ratios in the range 0.96–1.1. The cathodic peak current was found to be linearly related (with zero intercept) to the square root of the scan rate between 1 and 100 V/s.

From the above it may be concluded that the reduction processes under study are not complicated by adsorption phenomena or coupled chemical reactions. Accordingly, the mean of the cathodic and anodic peak potentials ($E_{1/2}$) is a good estimation of the formal reduction potential of the complexes. The observed $E_{1/2}$ fall in the range -0.001 to 0.117 V (Table 7). Neutral derivatives are significantly more reducible than the corresponding anionic species. No apparent changes in the redox potential result from the substitution of a DMSO for a TMSO ligand.

According to the measured $E_{1/2}$, a biological reduction process is thermodynamically possible for all the derivatives [17]. In this respect it is interesting to compare the $E_{1/2}$ value of **5b** with that of **ICR**, which we found to be -0.511 V under the same conditions. This last value sits at the lower limit of the biologically accessible potentials suggesting that, in the hypothesis of an 'activation by reduction' mechanism operating *in vivo* for these Ru(III) complexes, the sulfoxide derivatives might be expected to behave quite differently from **ICR** despite their structural similarity.

For the anionic derivatives with H_2O, Im, MeIm, NH_3, Pz and Py it is possible to compare the observed $E_{1/2}$ value with that calculated according to the linear relation given by Lever for Ru(III)/Ru(II) couples in water (Fig. 6) and based on his electrochemical ligand parameters E_L [40]. As it may be seen, the predicted redox potentials are considerably lower than those observed. Even though the range of $E_{1/2}$ values in our hands is too narrow to attempt any reasonable correlation, yet there are at least two factors to be considered when comparing our results with Lever's prediction. On one hand, Lever's correlation in water was based essentially on Ru(II) species with a +2 net charge, while our complexes have a net -2 charge for the same oxidation state. Actually, one would expect this to push the formal potentials towards more negative values. On the other hand, the high affinity of the DMSO ligand for Ru(II), together with its rather strong π-acidic character stimulated by the abundance of

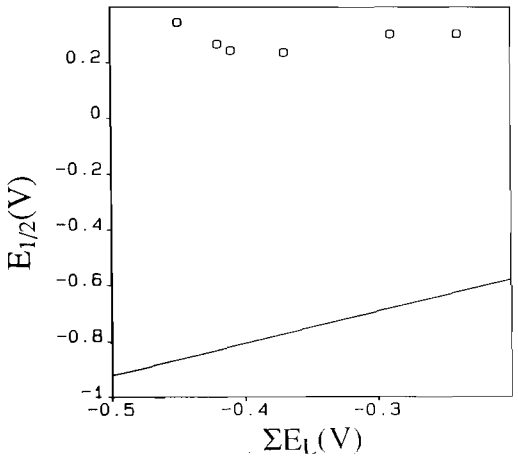

Fig. 6. Observed $E_{1/2}$ values (vs. NHE) for the anionic complexes with H_2O, Im, MeIm, NH_3, Pz and Py vs. the corresponding Lever's ΣE_L. The straight line is drawn according to Lever's correlation: $E_{1/2} = 1.14(\Sigma E_L) - 0.35$; for the construction of the figure, the $E_{1/2}$ values were referred to the NHE by assuming E(SSCE) vs. NHE = 0.236 V [41].

negative charge in the complexes, act in the opposite direction, moving the formal potentials towards more positive values. As a matter of fact, substitution of an imidazole ligand for a DMSO (cf. **ICR** and **5b**), induces an increase in the reduction potential of 0.51 V (see above). Moreover, in a previous paper [15] we found that the electrochemical behaviour of the parent compounds **1Na** and **2** is heavily influenced by the peculiar character of the DMSO ligand. Finally, a similar extra-stabilization effect due to π-acidic ligands has been recently reported for similar complexes [42].

As an alternative hypothesis, in aqueous solution the complexes might be in rapid equilibrium with some other species which actually undergo reduction at the electrode surface (CE mechanism). According to the independent NMR evidence, however, the concentration of such electroactive species should be below the limit of detection and we can estimate 5×10^{-2} as the maximum value for their formation equilibrium constant. Since all the cyclic voltammograms remain unchanged up to a scan rate of 100 V/s, a lower limit of about 7.5×10^6 s^{-1} can be derived for the first order rate constant pertinent to the formation of the electroactive species from the complexes. This, in turn, determines a lower bound of 1.5×10^8 s^{-1} of the rate constant for the opposite reaction. Actually, this last value seems to be very high, even if this mechanistic hypothesis cannot be conclusively excluded.

Conclusions

The two new classes of ruthenium(III) derivatives reported in this paper fulfill the basic requirement that prompted their synthesis. In fact, as shown by preliminary results, they have an increased inertness in aqueous solution compared to their precursors. We attribute this behaviour to the reinforcement of the Ru–DMSO bond which, according to both structural (Ru–S and S–O bond distances) and spectroscopic (S=O stretching frequencies) results, is due to an increased π back-bonding contribution. The presence of coordinated sulfoxide is also fundamental in determining the ease of reduction of the complexes through a stabilization of the Ru(II) oxidation state.

A thorough investigation of the chemical behaviour of the complexes in aqueous solution, with particular regard to physiological conditions, is currently in progress.

The two new classes of compounds will allow also a rather systematic approach to the study of the antitumor properties of ruthenium compounds, due to the possibility of exploring a range of chemical and physicochemical properties (e.g. solubility, lipophilicity, redox potential) while maintaining unaltered the complex structure. Some preliminary results on the antitumor activity of selected compounds, in comparison with **ICR**, are already available in the literature [43, 44].

Supplementary material

Elemental analysis of the complexes whose synthesis was not explicitly reported, anisotropic thermal parameters, hydrogen atom coordinates and tables of observed and calculated structure factors are available on request from the authors.

Acknowledgements

Financial support from M.U.R.S.T. (Rome) is gratefully acknowledged as well as the I.C.T.P. (Trieste) for a research fellowship to W.M.A. The authors are grateful to Dr L. G. Marzilli (Emory University, Altanta, USA) for access to the NMR spectrometer and to Dr K. A. Keating (Emory University) for helpful discussion and suggestions concerning the NMR of paramagnetic complexes. The help of F. Todone (Trieste) in the synthesis of some compounds is also acknowledged.

References

1 J. D. Gilbert, D. Rose and G. Wilkinson, *J. Chem. Soc. A*, (1970) 2765.
2 P. G. Antonov, Yu. N. Kukushkin, V. I. Konnov and B. I. Ionin, *Russ. J. Inorg. Chem. (Engl. Transl.)*, *23* (1978) 245.

3 (a) T. Bora and M. M. Singh, *Russ. J. Inorg. Chem. (Engl. Transl.), 20* (1975) 231; (b) *J. Inorg. Nucl. Chem., 38* (1976) 1815; (c) *Transition Met. Chem. (Weinheim Ger.), 3* (1978) 27.

4 (a) U. C. Sarma, K. P. Sarma and R. K. Poddar, *Polyedron, 7* (1988) 1727; (b) U. C. Sarma and R. K. Poddar, *Polyhedron, 7* (1988) 1737.

5 I. P. Evans, A. Spencer and G. Wilkinson, *J. Chem. Soc., Dalton Trans.,* (1973) 204.

6 J. S. Jaswal, S. J. Rettig and B. R. James, *Can. J. Chem., 68* (1990) 1808.

7 E. Alessio, B. Milani, M. Calligaris and N. Bresciani-Pahor, *Inorg. Chim. Acta, 194* (1992) 85.

8 E. Alessio, G. Balducci, M. Calligaris, G. Costa, W. M. Attia and G. Mestroni, *Inorg. Chem., 30* (1991) 609.

9 M. Calligaris, N. Bresciani-Pahor and R. S. Srivastava, *Acta Crystallogr., Sect. C,* in press.

10 E. Alessio, B. Milani, G. Mestroni, M. Calligaris, P. Faleschini and W. M. Attia, *Inorg. Chim. Acta, 177* (1990) 255.

11 (a) G. Sava, S. Zorzet, T. Giraldi, G. Mestroni and G. Zassinovich, *Eur. J. Cancer Clin. Oncol., 20* (1984) 841; (b) E. Alessio, W. M. Attia, M. Calligaris, S. Cauci, L. Dolzani, G. Mestroni, C. Monti-Bragadin, G. Nardin, F. Quadrifoglio, G. Sava, M. Tamaro and S. Zorzet, in M. Nicolini (ed.), *Platinum and Other Metal Coordination Compounds in Cancer Chemotheraphy,* Martinus Nijhoff, Boston, MA, 1988, p. 617; (c) G. Mestroni, E. Alessio, M. Calligaris, W. M. Attia, F. Quadrifoglio, S. Cauci, G. Sava, S. Zorzet, S. Pacor, C. Monti-Bragadin, M. Tamaro and L. Dolzani, *Progress in Clinical Biochemistry and Medicine,* Vol. 10, Springer, Berlin, 1989, p. 71; (d) G. Mestroni, E. Alessio, G. Sava, S. Pacor and M. Coluccia, in B. K. Keppler (ed.), *Metal Complexes in Cancer Chemotherapy,* VCH, Weinheim, 1993, in press.

12 E. Alessio, G. Mestroni, G. Nardin, W. M. Attia, M. Calligaris, G. Sava and S. Zorzet, *Inorg. Chem., 27* (1988) 4099.

13 E. Alessio, Y. Xu, S. Cauci, S. G. Mestroni, F. Quadrifoglio, P. Viglino and L. G. Marzilli, *J. Am. Chem. Soc., 111* (1989) 7066.

14 M. Henn, E. Alessio, G. Mestroni, M. Calligaris and W. M. Attia, *Inorg. Chim. Acta, 187* (1991) 39.

15 G. Costa, G. Balducci, C. Tavagnacco, E. Alessio and G. Mestroni, *J. Electroanal. Chem. Interfacial Electrochem., 296* (1990) 57.

16 (a)B. K. Keppler, W. Rupp, U. M. Juhl, H. Endres, R. Niebl and W. Balzer, *Inorg. Chem., 26* (1987) 4366; (b) F. T. Garzon, M. R. Berger, B. K. Keppler and D. Schmähl, *Cancer Chemother. Pharmacol., 19* (1987) 347; (c) B. K. Keppler, *Progress in Clinical Biochemistry and Medicine,* Vol. 10, Springer, Berlin, 1989, p. 41; (d) B. K. Keppler, M. R. Berger and M. E. Heim, *Cancer Treat. Rev., 17* (1990) 261.

17 M. J. Clarke, *Progress in Clinical Biochemistry and Medicine,* Vol. 10, Springer, Berlin, 1989, p. 25.

18 (a) P. K. L. Chan, P. K. H. Chan, D. C. Frost, B. R. James and K. A. Skov, *Can. J. Chem., 66* (1988) 117; (b) P. K. L. Chan, B. R. James, D. C. Frost, P. K. H. Chan and H. L. Hu, *Can. J. Chem., 67* (1989) 508.

19 D. Britz, *Electrochim. Acta, 25* (1980) 1449.

20 *International Tables for X-ray Crystallography,* Vol. IV, Kynoch, Birmingham, U.K., 1974.

21 *Enraf-Nonius Structure Determination Package,* B. A. Frenz & Associates, Enraf-Nonius, Delft, The Netherlands, 1985.

22 W. L. Reynolds, *Prog. Inorg. Chem., 12* (1970) 1.

23 C. V. Senoff, E. Maslowsky Jr. and R. G. Goel, *Can. J. Chem., 49* (1971) 3585.

24 R. S. McMillan, A. Mercer, B. R. James and J. Trotter, *J. Chem. Soc., Dalton Trans.,* (1975) 1006.

25 Yu. V. Fadeev, Yu. N. Kukushkin and K. A. Khokhryakov, *Russ. J. Inorg. Chem., 20* (1975) 1519.

26 J. A. Davies, *Adv. Inorg. Chem. Radiochem., 24* (1981) 115.

27 G. A. Heath, A. J. Lindsay and T. A. Stephenson, *J. Chem. Soc., Dalton Trans.,* (1982) 2429.

28 H. Toi, G. N. La Mar, R. Margalit, C. M. Che and H. B. Gray, *J. Am. Chem. Soc., 106* (1984) 6213.

29 H. C. Stynes and J. A. Ibers, *Inorg. Chem., 10* (1971) 2304.

30 F. C. March and G. Ferguson, *Can. J. Chem., 49* (1971) 3590.

31 P. J. M. W. L. Birker and P. T. Beurskens, *Recl. Trav. Pays-Bas, 93* (1974) 218.

32 R. P. Mason and J. E. Harriman, *J. Chem. Phys., 65* (1976) 2274.

33 J. Buchanan, E. J. M. Hamilton, D. Reed and A. J. Welch, *J. Chem. Soc., Dalton Trans.,* (1990) 677.

34 B. R. James, R. H. Morris, F. W. B. Einstein and A. Willis, *J. Chem. Soc., Chem. Commun.,* (1980) 31.

35 B. Viossat, P. Khodadad and N. Rodier, *J. Mol. Struct., 71* (1981) 237.

36 W. Feder, H. Dreizler, H. D. Rudolph and W. Typke, *Z. Naturforsch., Teil A, 24* (1969) 266.

37 W. J. J. Smeets, A. L. Spek, F. G. M. Niele, C. F. Martens and R. J. Nolte, *Acta Crystallogr., Sect. C, 43* (1987) 2330.

38 A. J. Blake, J. A. Grieg and M. Schroder, *Acta Crystallogr., Sect. C, 46* (1990) 322.

39 C. George and D. S. Dudis, *Acta Crystallogr., Sect. C, 46* (1990) 650.

40 A. B. P. Lever, *Inorg. Chem., 29* (1990) 1271.

41 A. J. Bard and L. R. Faulkner, *Electrochemical Methods,* Wiley, New York, 1980.

42 C. M. Duff and R. A. Schmid, *Inorg. Chem., 30* (1991) 2938.

43 S. Pacor, G. Sava, V. Ceschia, F. Bregant, G. Mestroni and E. Alessio, *Chem-Biol. Interact., 78* (1991) 223.

44 G. Sava, S. Pacor, G. Mestroni and E. Alessio, *Anti-Cancer Drugs, 3* (1992) 25.